Published in final edited form as:
Lab Chip. 2009 January 7; 9(1): 97–106. doi:10.1039/b809590f.

Microfluidic Device for Multimodal Characterization of Pancreatic Islets

Javeed Shaikh Mohammed[1], **Yong Wang**[2], **Tricia A. Harvat**[2], **Jose Oberholzer**[1,2], and **David T. Eddington**[1,3]

[1]Department of Bioengineering, University of Illinois at Chicago, Chicago, IL

[2]Department of Surgery, University of Illinois at Chicago, Chicago, IL

[3]Department of Biopharmaceutical Sciences, University of Illinois at Chicago, Chicago, IL

Abstract

A microfluidic device to perfuse pancreatic islets while simultaneously characterizing their functionality through fluorescence imaging of the mitochondrial membrane potential and intracellular calcium ($[Ca^{2+}]_i$) in addition to enzyme linked immunosorbent assay (ELISA) quantification of secreted insulin was developed and characterized. This multimodal characterization of islet function will facilitate rapid assessment of tissue quality immediately following isolation from donor pancreas and allow more informed transplantation decisions to be made which may improve transplantation outcomes. The microfluidic perfusion chamber allows flow rates of up to 1 mL/min, without any noticeable perturbation or shear of islets. This multimodal quantification was done on both mouse and human islets. The ability of this simple microfluidic device to detect subtle variations in islet responses in different functional assays performed in short time-periods demonstrates that the microfluidic perfusion chamber device can be used as a new gold standard to perform comprehensive islet analysis and obtain a more meaningful predictive value for islet functionality prior to transplantation into recipients, which is currently difficult to predict using a single functional assay.

INTRODUCTION

Diabetes Mellitus (DM) is a group of metabolic disorders in which the body does not regulate blood glucose levels properly, resulting in elevated levels of blood glucose. There are two major types of DM: Type I and II. Type I DM is an autoimmune disease which involves the destruction of β-cells (insulin secreting cells in islets of Langerhans) leading to insulin deficiency.[1] In Type II DM, insulin (a key regulator of carbohydrate metabolism) is produced but there is insulin resistance in peripheral tissues (such as adipose and muscle), and at later stages of Type II DM, insulin secretion is damaged because of glucotoxicity and lipotoxicity. For Type I DM, maintaining blood glucose levels under tight control with exogenous insulin injection represents the most effective way to prevent the onset or to reduce progression of the chronic complications. Currently, intensive insulin therapy has shown to reduce most complications associated with Type I DM patients,[2, 3] however, it can never approximate pulsatile insulin secretory patterns[4–7] of the normal β-cell and comes with risks of major hypoglycemic episodes. Whole pancreas transplantation was the only therapeutic modality that can stop the progression of diabetic complications without increasing the incidence of hypoglycemic events. Unfortunately, the procedure has a high morbidity and significant mortality rate.[8]

Correspondence to: David T. Eddington.

In the year 2000, the Edmonton group reported a series of 7 patients reaching insulin-independence after islet transplantation from multiple donors using steroid-free, sirolimus based immunosuppression. With the new protocol, islet transplantation is progressively becoming a promising treatment for Type I DM with benefits of minimal surgery, less mortality and morbidity.[9–13] In brief, the donated pancreas from a cadaver is digested by collagenase and then further purified by continuous Biocoll gradients. After short culture period, islets are transplanted into the liver via the portal vein system. Currently, prior to transplantation, the islets are put through a rigorous quality control to assess their purity, morphology, sterility, pyrogenicity, viability, and potency (static glucose-stimulation studies).[9, 14] However, the standard assays for evaluating islet quality prior to transplantation such as static glucose incubation and viability assay provide us with little information about β-cell function and does not address defects in β-cell morphology, metabolism, and signaling levels. Transplantation of isolated islets to diabetic nude mice models has been used as an in vivo model to assess the islet potency (ability of the transplanted islets to reverse DM). The time to reverse DM and the proportion of mice in which DM reverses provides potency of that batch of islets. This information along with glucose tolerance tests allows in predicting the efficiency of transplanted islets in the recipient, but in retrospect manner as the mouse model takes as long as 45 days. Therefore, it is essential to develop a standardized, accurate, real-time assessment of β-cell function based on β-cell physiology that can be used as a gold standard for assessing the functionality of islet preparations post isolation prior to transplantation.[14, 15] In this paper we present the design, fabrication, and testing of a microfluidic device for multiplexing several well-accepted islet functional assays.

Temporally resolved analysis of the kinetics of insulin secretion, mitochondria potential, and $[Ca^{2+}]_i$ will provide in depth understanding of the functionality of the islets. While all of these assays can be currently be multiplexed in a 96-well plate, these experiments rely on static incubation of the islets. The static analysis of islets can not provide the details on temporal dynamics of insulin secretion of islets and therefore necessitates dynamic perfusion of islets to obtain comprehensive information on the islets. Glucose-dependent islet signaling begins with uptake of glucose that is rapidly phosphorylated by glucokinase and converted to pyruvate by the glycolytic pathway, and then oxidized within the mitochondria by the tricarboxylic acid cycle and oxidative phosphorylation. Glucose catabolism generates ATP that consequently closes ATP-sensitive K^+ (K_{ATP}) channels, initiating plasma membrane depolarization, and increases $[Ca^{2+}]_i$. through the voltage-dependent calcium channel. As a result, the glucose-stimulated rise in $[Ca^{2+}]_i$ and insulin secretion are tightly coupled.[16] Previous studies[17] in conjunction with our laboratory observations indicate that mitochondrial damage, insulin degranulation, and cell surface membrane defects play key roles in determining human β-cell function and viability. The glucose-stimulated insulin secretion exhibits a biphasic response, an initial burst of insulin followed by a sustained basal level of insulin release. The first phase is characterized by a transient increase in insulin release that occurs 1–3 minutes after glucose stimulation and is 3–5 minutes in duration and then the second phase where insulin secretion decreases to a suprabasal level and gradually increases as long as the stimulating concentration of glucose is present. Loss of glucose-stimulated biphasic insulin secretion of islets has been observed in some diabetic mice models. Static incubation only provides the information of bulk insulin secretion (secretory capacity)[9] during the glucose-exposed period and will not reveal any information on the biphasic response. As the static glucose assay is currently the gold standard of islet characterization prior to transplantation, an incomplete assessment of islet functionality may result in poor transplantation outcomes.[18] In summary, current standard assays for evaluating human islet functionality prior to transplantation does not provide adequate information about human islet function and defects caused by organ procurement, cold ischemia, and islet isolation process. Therefore, a simple, quick, and predictable method to

evaluate human islets prior to transplantation would prove immensely useful to address these shortcomings.

Microfluidics offers a practical solution to this unmet clinical need to rapidly asses islet function.[19] Parallel microchannels enable multiple experiments to be performed simultaneously and imaging of cells within the microchannels, which is currently not possible with current commercially available dynamic perfusion platforms. Additionally, microfluidic delivery of stimulatory solutions reduces the mechanical perturbation that will reduce stress to the islets. Microfluidic assessment of islet function has been previously demonstrated including continuous perfusion and online electrophoresis immunoassay to study single[20, 21] and multiple (four)[19] mouse islets, for automated sampling,[22] fluorogenic labeling,[18] capillary electrophoresis analysis of islet proteins,[21, 23] and for partially stimulating mouse islets allowing observation of the NAD(P)H and individual β-cell $[Ca^{2+}]_i$ responses.[7] However, none have aimed to provide a simple device to characterize the kinetics of insulin secretion through imaging and collecting the perfusate for off-chip analysis in a platform designed to plug into the already complex transplantation arena. While these devices have demonstrated new biological insight and offer unique advantages not possible with current techniques, they also share complex designs and require expert users to operate. To successfully deploy a device at multiple transplantation centers, the device must be simple, robust, user-friendly, and provide quick, reproducible results that are predictive of transplant outcome;[15] as a device failure during a characterization process may lead to discarding potentially lifesaving donor tissue. We have developed a new device to simultaneously quantify the mitochondrial potential, $[Ca^{2+}]_i$ and biphasic response of islets in response to dynamic glucose stimulation to provide a complete assessment of islet function.[9, 18] Multimodal islet characterization experiments can be rapidly preformed within the islet isolation arena to directly assess tissue function without sacrificing valuable tissue or time. The microfluidic device consists of three layers (one with tiny circular wells, another with a large circular well, and a layer with rectangular microchannel) of polydimethylsiloxane (PDMS), and contains six identical perfusion chambers for assay multiplexing. Figure 1a contains the cross-sectional and isometric view of a single perfusion chamber. In each chamber, the bottom-most layer consists of an array of tiny circular wells that help to gently immobilize the islets without shielding them from the perfusion fluids to maximize the amount of islet surface area exposed to flow. The diameter and depth of the wells are 500 μm and 150 μm, respectively. Each well is separated from another well by 60 μm. It has been confirmed that the well design can successfully immobilize the islets with a size range from 50–500 μm at flow rate as large as 1 mL/min. Use of high flow rates prevents build up of high concentrations of insulin within the perfusion chamber before being washed out.[19] The next layer is a 7 mm diameter by 3 mm deep circular well that encompasses the array of the tiny wells. The top-most layer is a rectangular microchannel that feeds into the larger well. The channel introduces the perfusate at one of end of the large well and collects it from the opposite end of the well. The dimensions of the channel are 19 mm × 2 mm × 500 μm. The height of the channels was chosen to be 500 μm in order to accommodate the expected largest size of human islets. The simple design of the perfusion chamber allows the use of the microfluidic device for multiple experiments after simple cleaning procedure with alcohol and DI water; also, the soft lithography processes used to fabricate the device facilitate easy replication of devices. The device design leverages previously proven microfluidic techniques and is in itself not novel, however, multimodal characterization assays of islet tissue is a new and exciting application that will have a real and immediate impact in the transplantation clinic.

MATERIALS AND METHOD

Fabrication of the microfluidic device

Figure 2 depicts the fabrication flow used for the microfluidic perfusion chamber. Standard SU8 lithography was used to create the masters for the array of small wells and the rectangular channels as previously described.[24] Briefly, silicon wafers (3-inch) were cleaned in acetone, methanol, isopropanol and dried in a stream of N_2. The wafer was then exposed to oxygen plasma for 30 s at a power of 425 W (Terra Universal) to oxidize any remaining organics. Next, SU8 was spun on the cleaned silicon wafer for 30 seconds at 2000 rpm (SU8–100) or 1000 rpm (SU8–2150) to achieve thicknesses of 150 μm and 500 μm, respectively. The wafer was then exposed and developed to achieve a mold master.

Device characterization

Fluorescence intensity of perfused solutions was measured over time across different regions in the perfusion chamber to assess the ability of the device to switch perfused solutions in the chamber. DI water was perfused for 30 s, followed by fluorescein isothiocyanate (2 μM FITC, Sigma, MO) for 60 s, and finally flushing out the fluorescein with DI water at a flow rate of 1 mL/min. Images were collected with a high-speed, high-resolution charge-coupled device (CCD) (Retiga-SRV, Fast 1394, QImaging) and analyzed using image processing (SlideBook 4.2, Olympus).

Islet isolation and culture

Mouse pancreatic islets were isolated and cultured as previously described.[25] In brief, the pancreata of 8–10 week-old C57/B6 or BALB/c (Jackson Laboratory) were perfused with 0.22 mg/mL Collagenase (Sigma, MO) and then digested for 11 minutes at 37 °C. The digested pancreata were shaken vigorously for 15 seconds and further purified through discontinuous Ficoll gradient. The purified islets were cultured in 95% air and 5% CO_2 at 37 °C with RPMI-1640 medium supplemented with 10% fetal bovine serum. All procedures were approved by the Animal Care and Use Committee at the University of Illinois at Chicago.

Human islets were isolated and purified using the standard Edmonton protocol at the University of Illinois at Chicago (UIC) following informed consent by donor relatives. The pancreata were digested using a modified automated method as described previously[14, 26] and further purified by continuous gradients on a cell separator (COBE 2991TM, COBE Laboratories Inc, Lakewood, CO) at 4 °C and then cultured at 37 °C.

Experimental setup for perfusion and imaging

Two multi-syringe infusion pumps (Harvard Apparatus) were used to supply different solutions at the inlet of each microfluidic perfusion chamber. One pump was used to supply basal glucose solution to the perfusion chambers and the other pump was used to supply either stimulatory glucose, potassium chloride (KCl), tolbutamide (TB), or alpha-ketoisocaproate (KIC) solutions. All the input solutions were pre-warmed to 37 °C until used. A flow rate of 1 mL/min was set for both the pumps to achieve adequate volume for later analysis. Bovine serum albumin is first injected through the device to coat the channel walls to prevent non-specific insulin adsorption. All experiments were performed at 37 °C. Figure 1a shows the experimental setup used for this work.

Islet loading into the device

The islets are introduced into the access ports in the microfluidic chamber using a micropipette. For mouse islet experiments 25 islets were introduced into each perfusion

chamber and for human islet experiments 100 islets were introduced. The islets are introduced from one of the access ports of the perfusion chamber. Care was taken while introducing the islets into the perfusion chamber to prevent rupturing of islets. When the microfluidic device is tilted, the islets roll down along the microchannel and fall into the large circular well and eventually the islets (represented by the spheres in Figure 1a) settle down into the smaller circular wells at the bottom of the large circular well. After the islets have been introduced into the perfusion chambers, the inlet and outlet tubing were integrated with the microfluidic device using connectors. To eliminate any effects of manual handling, the islets are again perfused with 2 mM basal glucose solutions for 10–15 minutes before starting any experiments.

Dynamic perfusion of islets

Dynamic glucose stimulation of islets was achieved by exposing islets to steps in glucose concentrations while collecting the perfusate for quantifying the amount of secreted insulin using a standard ELISA kit. The microfluidic perfusion chambers were loaded with 25 mouse islets and each perfusion chamber was perfused with 2 mM basal glucose solution for 10–15 minutes prior to the start of collecting data as described above. After this initial phase 2 mM basal glucose solution was perfused for an additional 5 minutes and stimulatory glucose solution (8 mM, 12 mM, 16.7 mM glucose solutions in separate channels) for 20 minutes, followed by 2 mM basal glucose solution for another 5 minutes. The perfusate from each chamber was collected in centrifuge tubes and ELISA assay was performed.

As islets range from 50–500 μm in diameter, they easily settle in the 500 μm diameter wells. It was observed that with this device design, even at a flow rate of 1 mL/min there was no noticeable perturbation or shear of islets. The islets were stationary for long periods of time even during switching of fluids at the inlet port of the perfusion chamber facilitating time-lapse imaging of multiple islets.[27]

Calcium Imaging

Dual-wavelength excitation microfluorometry was used to measure $[Ca^{2+}]_i$ as described previously.[25] Islets were loaded with 5 μM Fura-2/AM (Molecular Probes Inc., Eugene, OR) through a 25 min incubation at 37 °C in Krebs-Ringer buffer (KRB) solution with 2 mM glucose (KRB2), then loaded into the microfluidic perfusion device and mounted on an inverted epifluorescence microscope (IX71, Olympus) equipped with a heating stage and perfused by a continuous flow (1 mL/min) of KRB2 at 37 °C (pH 7.4). KRB containing different glucose concentrations were administered to the islets after rinsing in KRB2 for 10–15 min. Multiple islets were simultaneously imaged with 10×–20× objectives. Fura-2 dual-wavelength excitation at 340 and 380 nm (shift in excitation wavelength occurs upon binding Ca^{2+}),[28] and detection of fluorescence emission at 510 nm was accomplished using an image acquisition and analysis software (SlideBook 4.2, Olympus); images were collected with a high-speed, high-resolution charge-coupled device (Retiga-SRV, Fast 1394, QImaging). The images were acquired near the equatorial plane of the islets. As the handpicked islets were of similar size, the equatorial plane of all the islets being imaged was approximately the same. All experiments were performed at 37 °C. Once the software settings were set for Fura-2 dual excitation imaging, the islets were perfused with KRB2 for 5 minutes, 14 mM glucose solution for 15 minutes, KRB2 for another 10 minutes, 30 mM KCl solution for 10 minutes and finally with KRB2 for 5 minutes. The perfusate was collected for Insulin ELISA.

Mitochondria Potential Imaging

Rhodamine 123 (Rh123) was used as an indicator of mitochondrial membrane potential. Rh123 is a lipophilic cation that partitions selectively into the negatively-charged

mitochondrial membrane. Hyper-polarization of the mitochondrial membrane causes uptake of Rh123 into mitochondria and a decrease in fluorescence due to intermolecular crowding and quenching.[25] Islets were incubated in KRB2 supplemented with 10 μg/mL Rh123 for 20 minutes at 37 °C, then loaded into the microfluidic perfusion device and mounted on an inverted epifluorescence microscope equipped with a heating stage and perfused by a continuous flow (rate 1 mL/min) of KRB2 at 37 °C (pH 7.4). KRB containing different glucose concentrations were administered to the islets after rinsing in KRB2 for 10–15 minutes. Rh123 fluorescence was excited at 540 nm and emission measured at 590 nm. Images were collected with a CCD as described above. Data was normalized to the average fluorescence intensity recorded during a five-minute period prior to glucose stimulation. All experiments were performed at 37 °C. Once the software settings were set for Rhodamine 123 imaging, the islets were perfused with KRB2 for 5 minutes, next with 14 mM glucose solution for 15 minutes, followed by KRB2 for 5 minutes. The perfusate was collected for Insulin ELISA.

Insulin ELISA method

The perfusate samples were frozen at −80 °C until quantification with the ELISA kit. Insulin was measured using Mammalian or Mice Insulin ELISA (Mercodia AB, Uppsala, Sweden) kits. The protocol provided by the manufacturer was followed.

RESULTS AND DISCUSSION

Figure 1b shows the fluorescence intensity of perfused solutions measured over time across different regions in the perfusion chamber during the perfusion of DI water and fluorescein solutions. The intensity values are area averages of three different scans. The intensity changes in the plots clearly illustrate the ability of the large circular well to completely exchange its stimulatory solution in approximately two minutes. The fluid flow within the perfusion chamber is an important factor in switching fluids with a step change and to provide uniform concentrations of fluids around the islets.[19] The loading of islets and the relative position of the islets being imaged within the perfusion chamber need to be standardized to obtain comparable results and can be improved in future iterations. After the characterization of the microfluidic device was done, it was applied to test different assays with mouse islets.

The glucose-stimulated insulin secretion in islets is coupled to the metabolic state of the β-cells and involves both glycolytic and Krebs cycle metabolism.[29] The stimulatory glucose is phosphorylated after it enters the cells and undergoes glycolysis leading to increased metabolic flux and closure of the plasma membrane-associated ATP-sensitive K^+ (K_{ATP}) channels.[29, 30] This channel closure in turn depolarizes the membrane leading to the activation of the voltage-sensitive Ca^{2+} channels and a concomitant rise in $[Ca^{2+}]_i$, and increased insulin secretion.[6, 7, 28, 29, 31–42] Mouse islets were dynamically perfused with basal and stimulatory glucose solutions and the secreted insulin profiles are shown in Figure 3a. From the plots it is clear that the microfluidic perfusion device successfully characterizes the biphasic insulin release profile of mouse islets; an initial sharp rise followed by a moderate elevation.[16, 18, 22, 28, 31, 43, 44] The mouse islets show a clear dose-response illustrated with a marked increase in the insulin secretion with increasing stimulatory glucose concentrations, and is consistent with previous reports.[25] There is slight delay in the onset of the peak after the islets are exposed to the stimulatory glucose consistent with previous reults.[18, 44]

After successfully applying the microfluidic device to perform dynamic glucose stimulation of mouse islets, the device was applied to perform simultaneous perfusion and imaging experiments. $[Ca^{2+}]_i$ imaging and insulin secretion analysis of mouse islets was performed

as this correlates to the functional capacity of the islets.45 We tracked the whole-islet $[Ca^{2+}]_i$ changes in multiple islets under basal and stimulatory glucose concentrations, and eventually under KCl stimulation. An absorption shift in excitation wavelength of Fura-2 loaded in the islets occurs upon binding of Ca^{2+}.[28] High extracellular KCl will collapse and depolarize the cell membrane leading to opening of voltage-dependent calcium, calcium influx, eventually insulin secretion.[46] Figure 3b contains the plot of temporal insulin secretion of the C57/B6 mice islets superimposed on the plot of temporal changes in ratio of the fluorescence intensities (340/380 nm) of the islets imaged. Figure 3c contains the plot of temporal insulin secretion of the BALB/c mice islets superimposed on the plot of temporal changes in ratio of the fluorescence intensities (340/380 nm) of the islets imaged. The secondary Ca^{2+} oscillations can be vividly seen in the Fura-2 plot, indicating that the device can successfully capture finer details of islet functionality. It is evident from the plots that the 14 mM stimulatory glucose and 30 mM KCl stimulation correlates to increased insulin secretion and $[Ca^{2+}]_i$ as expected.[25, 45] There is a time lag between the insulin release and Ca^{2+} release and can be ascribed to the limitations of the current system that will be addressed in future iterations (random location of islets in the perfusion chamber, diffusion of insulin, and flow within the chamber).[16] It is noteworthy that the time lag could partly be attributed to the time required for the $[Ca^{2+}]_i$ to reach the threshold to trigger exocytosis.[6, 28] Post-stimulation basal levels are very close to the pre-stimulation basal levels (as expected from the device characterization results), indicating that the stimulatory perfusion solutions exchanged properly inside the chamber.

In another set of simultaneous imaging and perfusion experiments, mitochondrial integrity and insulin secretion of mouse islets was evaluated as this correlates with functional capacity of the islets.[17] The mitochondrial membrane potential of β-cells is controlled by the ATP/ADP ratio through the K_{ATP} channel. Under stimulatory glucose, the ratio increases causing the depolarization of the β-cells and leading to insulin secretion. Rh123 (a lipophilic cation) partitions selectively into the negatively-charged mitochondrial membrane and hyper-polarization of the mitochondrial membrane causes uptake of Rh123 into mitochondria and a decrease in fluorescence due to intermolecular crowding and quenching.[25] Figure 3d contains the plot of temporal insulin secretion of the mouse islets superimposed on the plot of temporal changes in the fluorescence intensity (corresponding to the mitochondrial membrane potential) of the mouse islets imaged. It is evident from the plots that the 14 mM stimulatory glucose correlates to increased insulin secretion and decreased mitochondrial membrane potential as expected.[25] Here again, the post-stimulation basal levels are very close to the pre-stimulation basal levels, indicating that the stimulatory perfusion solutions exchanged properly inside the chamber.

After successful application of the microfluidic device to perform different assays on mouse islets, the device was applied to perform assays on human islets. Perfusion experiments were performed with 100 human islets as opposed to 25 mouse islets due to the relatively lower secreted insulin levels in human islets and higher variability of human islet function. Human islets were dynamically perfused with basal and stimulatory glucose solutions, and the representative secreted insulin profiles for a human pancreatic isolation batch is shown in Figure 4a. It is evident that the microfluidic perfusion device successfully characterizes the insulin release profile of human islets in response to step changes in glucose concentration; similar to the results observed with mouse islets. The human islets also show a clear dose-response illustrated with a marked increase in the insulin secretion with increasing stimulatory glucose concentrations, and is consistent with the results seen with mouse islets. Here again, a slight delay in the onset of the peak after the islets are exposed to the stimulatory glucose is seen.

Islets from different human pancreatic isolation batches have highly variable responses as opposed to more repeatable responses to islets from genetically similar experimental mice. Therefore, the results for human islets (in response to step changes in glucose concentration) from different human pancreatic isolation batches have been summarized in Table 1. Area under the curve (AUC) for insulin levels under 2 mM basal glucose (KRB2) followed by stimulation with 8, 12, 16.7 mM stimulatory glucose, and again under KRB2 in human islets have been presented separately for different human pancreatic isolation batches. It is clear from the data in Table 1 that although there is a distinct difference between basal and stimulatory insulin levels in all cases, there is a large batch-to-batch variability in responses to the different stimulatory glucose solutions. Also, the dose response to increasing glucose concentrations is not the same in all the batches. Another factor leading to the variability in the response could be due to multiple sizes of cells or inherent variability in cells.[28]

In another set of experiments, response of human islets to different commonly employed secretagogues (30 mM KCl, 150 μM TB, 10 mM KIC[34] in separate channels) was analyzed using the microfluidic device. Although these stimuli induce insulin secretion in islets, the mechanisms are different from the glucose induced insulin secretion. High extracellular KCl will collapse and depolarize cell membranes leading to opening of voltage-dependent calcium channels, calcium influx, and eventually insulin secretion.[46] TB is known as K^+-ATP channel blocker[16, 25, 30, 35] that causes the cells to depolarize and raise Ca^{2+} levels,[6, 36] there by making the cells secrete insulin.[38] TB is a sulphonylurea drug used to treat non-insulin-dependent DM patients.[6] KIC (mitochondrial fuel)[45] serves as a substrate for mitochondrial metabolism generating ATP and other signaling molecular independent of the glycolytic pathway.[5] Human islets were dynamically perfused with basal and secretagogue solutions and the representative secreted insulin profiles for a human pancreatic isolation batch is shown in Figure 4b. Our results clearly demonstrate that the microfluidic device can successfully characterize different islet physiological functions and produces repeatable and consistent data with mouse islets.[25, 30, 34, 45] The results for human islets (in response to step changes in different secretagogue solutions) from different human pancreatic isolation batches have been summarized in Table 2. AUC for insulin levels under KRB2 followed by stimulation with 30 mM KCl, 150 μM TB, 10 mM KIC, and again under KRB2 in human islets have been presented separately for different human pancreatic isolation batches. It is clear from the data in Table 2 that although there is a distinct difference between basal and stimulatory insulin levels in all cases, there is a large batch-to-batch variability in responses to the different secretagogue solutions; similar to the results for human islet responses to step changes in glucose solutions (Table 1).

The microfluidic device was next applied to perform simultaneous perfusion and imaging experiments with human islets. Representative results for a human pancreatic isolation batch is shown in Figure 4c that contains the plot of temporal insulin secretion of the human islets superimposed on the plot of temporal changes in ratio of the fluorescence intensities (340/380 nm) of the human islets imaged. It is evident from the plots that the 14 mM stimulatory glucose and 30 mM KCl stimulation correlates to increased insulin secretion and $[Ca^{2+}]_i$ as expected and consistent with mouse islets. The peaks are not as distinct and not as intense as observed in the case of mouse islets as it is known that the human islets have a wider range of mitochondrial membrane potential and $[Ca^{2+}]_i$ response to glucose as compared to mouse islets.[6] There is a time lag between the insulin release and Ca^{2+} release and can be ascribed to the limitations of the current system as previously mentioned. Post-stimulation basal levels are very close to the pre-stimulation basal levels as expected, indicating that the stimulatory perfusion solutions exchanged properly inside the chamber. The insulin secretion and $[Ca^{2+}]_i$ results for human islets from different human pancreatic isolation batches have been summarized in Table 3. AUC for FURA-2 ratio (representing $[Ca^{2+}]_i$) and insulin levels under KRB2, next by stimulation with 14 mM stimulatory

glucose, under KRB2, followed by stimulation with 30 mM KCl, and finally in KRB2 in human islets have been presented separately for different human pancreatic isolation batches. It is evident from the data in Table 3 that although there is a distinct difference between basal and stimulatory insulin levels in all cases, there is a large batch-to-batch variability in responses; similar to the previous human islet results (Table 1 and Table 2).

From the results it is evident that the microfluidic device will prove very useful in investigating islet physiology and drug action mechanisms on islets.[22, 38] The ability of this simple microfluidic device to detect subtle variations in islet responses in different functional assays performed in short time-periods demonstrates that the microfluidic perfusion chamber device can be used as a new gold standard to perform comprehensive islet analysis and obtain a more meaningful predictive value for islet functionality prior to transplantation into recipients, which is currently difficult to predict using a single functional assay. The authors understand that further experiments on multiple human islet tissue are required to statistically correlate these functional assays with transplantation outcomes; however the device presented here provides a simple route to collect this data. All the biochemical reactions involved in the functional assays utilize oxygen,[47–50] and the oxygen changes can be measured as oxygen consumption rate[15] can be used to improve the predictive power of islet functionality in future iterations. Islet function is currently being assessed by transplantation of isolated human islets to diabetic nude mice models. The long term in vivo transplantation results will be used as a benchmark to correlate the in vitro functional assay results.

CONCLUSIONS

In conclusion, we have developed a simple microfluidic device that can provide a comprehensive analysis of the functionality of islets prior to transplantation. We have successfully demonstrated that the microfluidic device can be used to perform multimodal islet functional assays. The different types of analyses that can be performed using this microfluidic device are not limited to the demonstrations presented in this paper. We intend to use this microfluidic device as a new gold standard to obtain an empirical relation between the different results obtained using multimodal functional assays to predict the islet transplantation efficiency in a time frame acceptable for the clinic.

Acknowledgments

Funding was provided to JO through National Institutes of Health (NIH) Center Grant, "Chicago Islet Consortium ICR at UIC" and by "The Chicago Project" to DTE through DARPA-BAA-07-21-FP-020 and the Alfred P. Sloan Foundation.

REFERENCES

1. Okubo Y, Shimada A, Kanazawa Y, Shigihara T, Oikawa Y, Imai T, Miyazaki J, Itoh H. Hyperplastic islets observed in "reversed" NOD mice treated without hematopoietic cells. Diabetes Res Clin Pract. 2008; 79(1):18–23. [PubMed: 17919765]
2. Diabetes Control and Complications Trial/Epidemiology of, D.; Interventions and Complications Research, G.; Retinopathy and nephropathy in patients with type 1 diabetes four years after a trial of intensive therapy. New England Journal of Medicine. 2000; 342(6):381–389. [PubMed: 10666428]
3. Keymeulen B, Vandemeulebroucke E, Ziegler AG, Mathieu C, Kaufman L, Hale G, Gorus F, Goldman M, Walter M, Candon S, Schandene L, Crenier L, De Block C, Seigneurin JM, De Pauw P, Pierard D, Weets I, Rebello P, Bird P, Berrie E, Frewin M, Waldmann H, Bach JF, Pipeleers D, Chatenoud L. Insulin needs after CD3-antibody therapy in new-onset type 1 diabetes. New England Journal of Medicine. 2005; 352(25):2598–2608. [PubMed: 15972866]

4. Lin JM, Sternesjo J, Sandler S, Bergsten P. Preserved pulsatile insulin release from prediabetic mouse islets. Endocrinology. 1999; 140(9):3999–4004. [PubMed: 10465269]
5. Lin JM, Fabregat ME, Gomis R, Bergsten P. Pulsatile insulin release from islets isolated from three subjects with type 2 diabetes. Diabetes. 2002; 51(4):988–993. [PubMed: 11916916]
6. Martin F, Soria B. Glucose-induced [Ca2+](i) oscillations in single human pancreatic islets. Cell Calcium. 1996; 20(5):409–414. [PubMed: 8955555]
7. Rocheleau JV, Walker GM, Head WS, McGuinness OP, Piston DW. Microfluidic glucose stimulation reveals limited coordination of intracellular Ca2+ activity oscillations in pancreatic islets. Proceedings of the National Academy of Sciences of the United States of America. 2004; 101(35):12899–12903. [PubMed: 15317941]
8. Gruessner AC, Sutherland DER. Pancreas transplant outcomes for United States (US) and non-US cases as reported to the United Network for Organ Sharing (UNOS) and the International Pancreas Transplant Registry (IPTR) as of October 2002. Clin Transpl. 2002:41–77. [PubMed: 12971436]
9. Inoue K, Miyamoto M. Islet transplantation. J Hepatobiliary Pancreat Surg. 2000; 7(2):163–177. [PubMed: 10982609]
10. Linn T, Schmitz J, Hauck-Schmalenberger I, Lai Y, Bretzel RG, Brandhorst H, Brandhorst D. Ischaemia is linked to inflammation and induction of angiogenesis in pancreatic islets. Clinical and Experimental Immunology. 2006; 144(2):179–187. [PubMed: 16634789]
11. Sigrist S, Mechine-Neuville A, Mandes K, Calenda V, Legeay G, Bellocq JP, Pinget M, Kessler L. Induction of angiogenesis in omentum with vascular endothelial growth factor: Influence on the viability of encapsulated rat pancreatic islets during transplantation. Journal of Vascular Research. 2003; 40(4):359–367. [PubMed: 12891005]
12. Fenjves ES, Ochoa MS, Gay-Rabinstein C, Molano RD, Pileggi A, Mendez AJ, Inverardi L, Ricordi C. Adenoviral gene transfer of erythropoietin confers cytoprotection to isolated pancreatic islets. Transplantation. 2004; 77(1):13–18. [PubMed: 14724429]
13. Reimer MK, Mokshagundam SP, Wyler K, Sundler F, Ahren B, Stagner JI. Local growth factors are beneficial for the autonomic reinnervation of transplanted islets in rats. Pancreas. 2003; 26(4): 392–397. [PubMed: 12717274]
14. Pileggi A, Ricordi C, Kenyon NS, Froud T, Baidal DA, Kahn A, Selvaggi G, Alejandro R. Twenty years of clinical islet transplantation at the Diabetes Research Institute--University of Miami. Clin Transpl. 2004:177–204. [PubMed: 16704150]
15. Sweet IR, Gilbert M, Scott S, Todorov I, Jensen R, Nair I, Al-Abdullah I, Rawson J, Kandeel F, Ferreri K. Glucose-stimulated increment in oxygen consumption rate as a standardized test of human islet quality. American Journal of Transplantation. 2008; 8:183–192. [PubMed: 18021279]
16. Gilon P, Shepherd RM, Henquin JC. Oscillations of Secretion Driven by Oscillations of Cytoplasmic Ca2+ as Evidenced in Single Pancreatic-Islets. Journal of Biological Chemistry. 1993; 268(30):22265–22268. [PubMed: 8226733]
17. Maechler P, Carobbio S, Rubi B. In beta-cells, mitochondria integrate and generate metabolic signals controlling insulin secretion. International Journal of Biochemistry & Cell Biology. 2006; 38(5–6):696–709. [PubMed: 16443386]
18. Roper MG, Shackman JG, Dahlgren GM, Kennedy RT. Microfluidic chip for continuous monitoring of hormone secretion from live cells using an electrophoresis-based immunoassay. Analytical Chemistry. 2003; 75(18):4711–4717. [PubMed: 14674445]
19. Dishinger JF, Kennedy RT. Serial immunoassays in parallel on a microfluidic chip for monitoring hormone secretion from living cells. Analytical Chemistry. 2007; 79(3):947–954. [PubMed: 17263320]
20. Tao L, Aspinwall CA, Kennedy RT. On-line competitive immunoassay based on capillary electrophoresis applied to monitoring insulin secretion from single islets of Langerhans. Electrophoresis. 1998; 19(3):403–408. [PubMed: 9551792]
21. Tao L, Kennedy RT. On line competitive immunoassay for insulin based on capillary electrophoresis with laser induced fluorescence detection. Analytical Chemistry. 1996; 68(22): 3899–3906. [PubMed: 8916449]
22. Shackman JG, Dahlgren GM, Peters JL, Kennedy RT. Perfusion and chemical monitoring of living cells on a microfluidic chip. Lab on a Chip. 2005; 5(1):56–63. [PubMed: 15616741]

23. Wu CH, Scampavia L, Ruzicka J. Micro sequential injection: automated insulin derivatization and separation using a lab-on-valve capillary electrophoresis system. Analyst. 2003; 128(9):1123–1130. [PubMed: 14529018]
24. Xia YN, Whitesides GM. Soft lithography. Annual Review of Materials Science. 1998; 28:153–184.
25. Avila JG, Wang Y, Barbaro B, Gangemi A, Qi M, Kuechle J, Doubleday N, Doubleday M, Churchill T, Salehi P, Shapiro J, Philipson LH, Benedetti E, Lakey JRT, Oberholzer J. Improved outcomes in islet isolation and transplantation by the use of a novel hemoglobin-based O-2 carrier. American Journal of Transplantation. 2006; 6(12):2861–2870. [PubMed: 17062000]
26. Salehi P, Hansen MA, Avila JG, Barbaro B, Gangemi A, Romagnoli T, Wang Y, Qi MG, Murdock P, Benedetti E, Oberholzer J. Human islet isolation outcomes from pancreata preserved with histidine-tryptophan ketoglutarate versus University of Wisconsin solution. Transplantation. 2006; 82(7):983–985. [PubMed: 17038916]
27. Lee PJ, Helman NC, Lim WA, Hung PJ. A microfluidic system for dynamic yeast cell imaging. Biotechniques. 2008; 44(1):91–5. [PubMed: 18254385]
28. Qian WJ, Peters JL, Dahlgren GM, Gee KR, Kennedy RT. Simultaneous monitoring of Zn2+ secretion and intracellular Ca2+ from islets and islet cells by fluorescence microscopy. Biotechniques. 2004; 37(6):922. [PubMed: 15597541]
29. Patterson GH, Knobel SM, Piston DW. Separation of the glucosestimulated cytoplasmic and mitochondrial NAD(P)H responses in pancreatic islet beta cells. Biophysical Journal. 2000; 78(1): 445A–445A.
30. Franklin I, Gromada J, Gjinovci A, Theander S, Wollheim CB. beta-Cell secretory products activate alpha-cell ATP-dependent potassium channels to inhibit glucagon release. Diabetes. 2005; 54(6):1808–1815. [PubMed: 15919803]
31. Valdeolmillos M, Nadal A, Contreras D, Soria B. The Relationship between Glucose-Induced K(Atp+) Channel Closure and the Rise in [Ca2+]I in Single-Mouse Pancreatic-Beta-Cells. Journal of Physiology-London. 1992; 455:173–186.
32. Kimple ME, Joseph JW, Bailey CL, Fueger PT, Hendry IA, Newgard CB, Casey PJ. G{alpha}z Negatively Regulates Insulin Secretion and Glucose Clearance. J Biol Chem. 2008; 283(8):4560–7. [PubMed: 18096703]
33. Gilon P, Henquin JC. Distinct Effects of Glucose on the Synchronous Oscillations of Insulin Release and Cytoplasmic Ca2+ Concentration Measured Simultaneously in Single-Mouse Islets. Endocrinology. 1995; 136(12):5725–5730. [PubMed: 7588329]
34. Macdonald MJ, Longacre MJ, Stoker SW, Brown LJ, Hasan NM, Kendrick MA. Acetoacetate and {beta}-hydroxybutyrate in combination with other metabolites release insulin from INS-1 cells and provide clues about pathways in insulin secretion. Am J Physiol Cell Physiol. 2008; 294(2):C442–C450. [PubMed: 18160486]
35. Nakada S, Ishikawa T, Yamamoto Y, Kaneko Y, Nakayama K. Constitutive nitric oxide synthases in rat pancreatic islets: direct imaging of glucoseinduced nitric oxide production in beta-cells. Pflugers Archiv-European Journal of Physiology. 2003; 447(3):305–311. [PubMed: 14564523]
36. Valdeolmillos M, Nadal A, Soria B, Garciasancho J. Fluorescence Digital Image-Analysis of Glucose-Induced [Ca2+](I) Oscillations in Mouse Pancreatic-Islets of Langerhans. Diabetes. 1993; 42(8):1210–1214. [PubMed: 8325454]
37. Trus M, Corkey RF, Nesher R, Richard AMT, Deeney JT, Corkey BE, Atlas D. The L-type voltage-gated Ca2+ channel is the Ca2+ sensor protein of stimulus-secretion coupling in pancreatic beta cells. Biochemistry. 2007; 46:14461–14467. [PubMed: 18027971]
38. Kim SW, Bae YH. Visual evidence and quantification of interaction of polymeric sulfonylurea with pancreatic islet. Biomacromolecules. 2003; 4(6):1550–1557. [PubMed: 14606879]
39. Kulkarni RN, Roper MG, Dahlgren G, Shih DQ, Kauri LM, Peters JL, Stoffel M, Kennedy RT. Islet secretory defect in insulin receptor substrate 1 null mice is linked with reduced calcium signaling and expression of sarco(endo)plasmic reticulum Ca2+-ATPase (SERCA)-2b and-3. Diabetes. 2004; 53(6):1517–1525. [PubMed: 15161756]

40. Deng Q, Kauri LM, Qian WJ, Dahlgren GM, Kennedy RT. Microscale determination of purines in tissue samples by capillary liquid chromatography with electrochemical detection. Analyst. 2003; 128(8):1013–1018. [PubMed: 12964599]
41. Rocheleau JV, Remedi MS, Granada B, Head WS, Koster JC, Nichols CG, Piston DW. Critical role of gap junction coupled K-ATP channel activity for regulated insulin secretion. Plos Biology. 2006; 4:221–227.
42. Remedi MS, Rocheleau JV, Tong A, Patton BL, McDaniel ML, Piston DW, Koster JC, Nichols CG. Hyperinsulinism in mice with heterozygous loss of K-ATP channels. Diabetologia. 2006; 49:2368–2378. [PubMed: 16924481]
43. Yada T, Sakurada M, Ihida K, Nakata M, Murata F, Arimura A, Kikuchi M. Pituitary Adenylate-Cyclase Activating Polypeptide Is an Extraordinarily Potent Intrapancreatic Regulator of Insulin-Secretion from Islet Beta-Cells. Journal of Biological Chemistry. 1994; 269(2):1290–1293. [PubMed: 8288592]
44. Fernandez-Pascual S, Mukala-Nsengu-Tshibangu A, del Rio RM, Tamarit-Rodriguez J. Conversion into GABA (gamma-aminobutyric acid) may reduce the capacity of L-glutamine as an insulin secretagogue. Biochemical Journal. 2004; 379:721–729. [PubMed: 14763900]
45. Zhou YP, Sreenan S, Pan CY, Currie KPM, Bindokas VP, Horikawa Y, Lee JP, Ostrega D, Ahmed N, Baldwin AC, Cox NJ, Fox AP, Miller RJ, Bell GI, Polonsky KS. A 48-hour exposure of pancreatic islets to calpain inhibitors impairs mitochondrial fuel metabolism and the exocytosis of insulin. Metabolism-Clinical and Experimental. 2003; 52(5):528–534. [PubMed: 12759879]
46. Zawalich WS, Zawalich KC. Effects of protein kinase C inhibitors on insulin secretory responses from rodent pancreatic islets. Molecular and Cellular Endocrinology. 2001; 177(1–2):95–105. [PubMed: 11377825]
47. Goto M, Holgersson J, Kumagai-Braesch M, Korsgren O. The ADP/ATP ratio: A novel predictive assay for quality assessment of isolated pancreatic islets. American Journal of Transplantation. 2006; 6(10):2483–2487. [PubMed: 16869808]
48. Papas KK, Pisania A, Wu H, Weir GC, Colton CK. A stirred microchamber for oxygen consumption rate measurements with pancreatic islets. Biotechnology and Bioengineering. 2007; 98:1071–1082. [PubMed: 17497731]
49. Fraker C, Montelongo J, Szust J, Khan A, Ricordi C. The use of multiparametric monitoring during islet cell isolation and culture: A potential tool for in-process corrections of critical physiological factors. Cell Transplantation. 2004; 13(5):497–502. [PubMed: 15565862]
50. Armann B, Hanson MS, Hatch E, Steffen A, Fernandez LA. Quantification of basal and stimulated ROS levels as predictors of islet potency and function. American Journal of Transplantation. 2007; 7(1):38–47. [PubMed: 17227556]

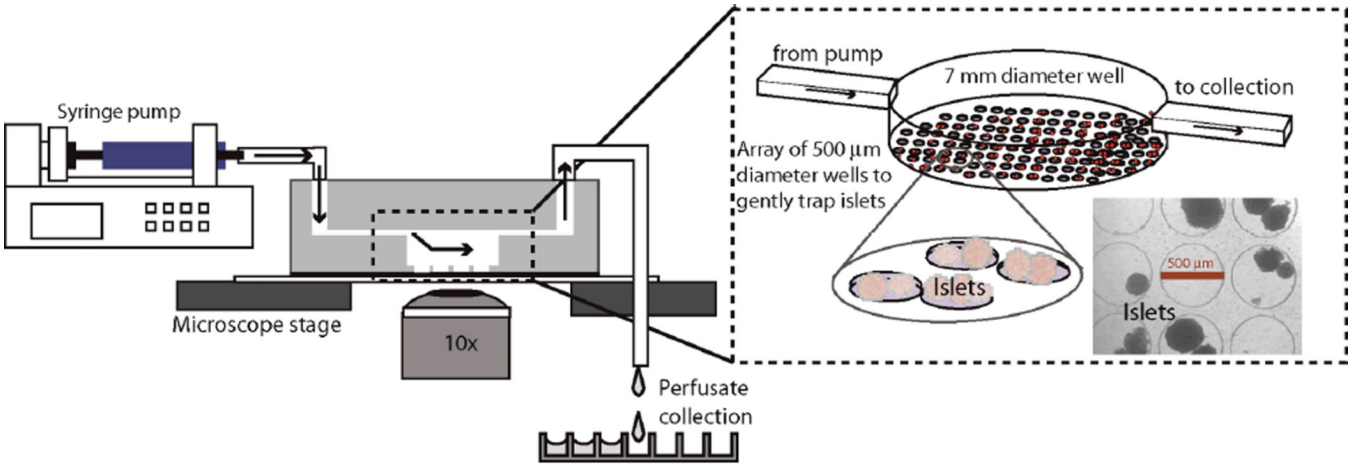

(a)

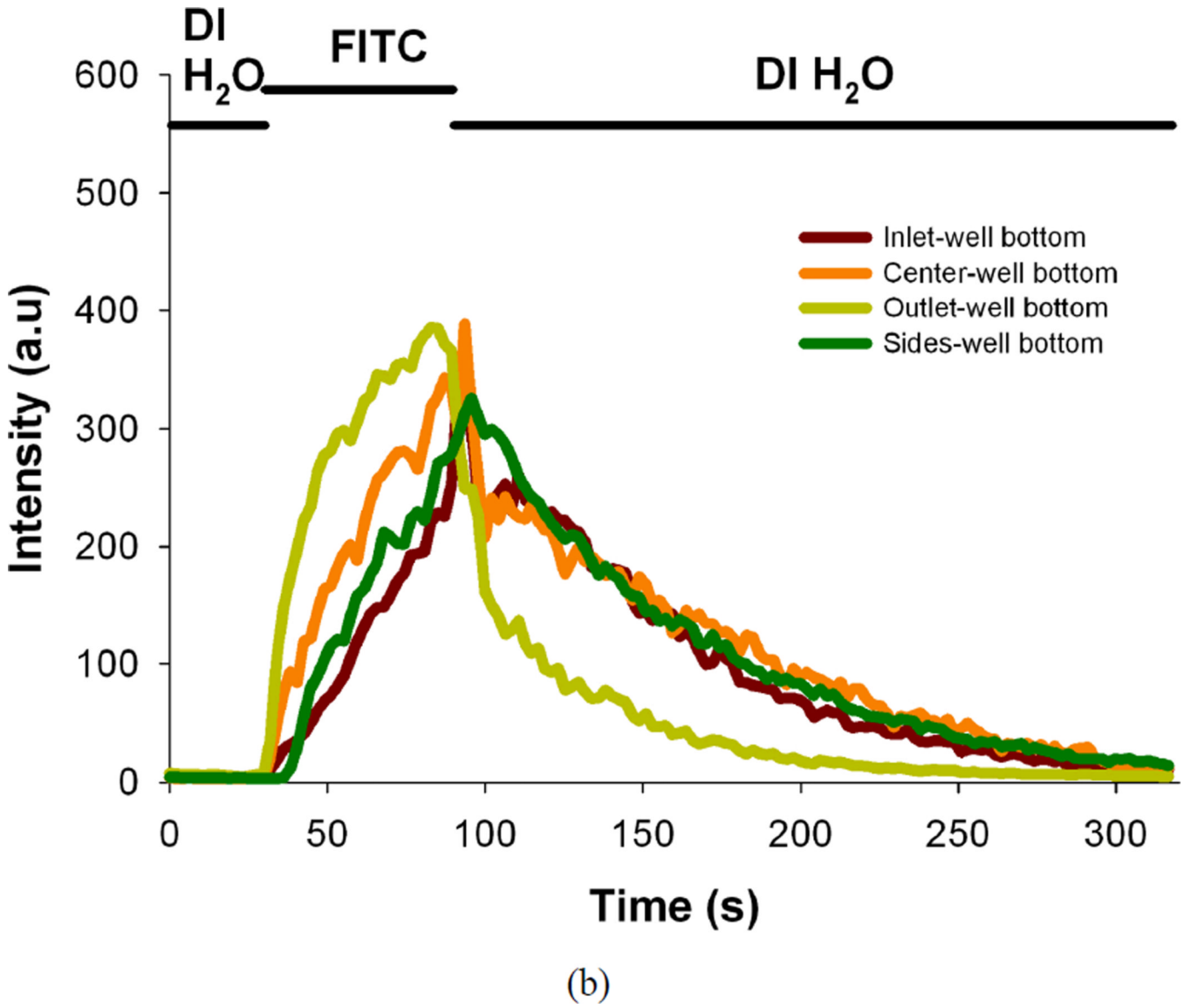

(b)

Figure 1.

(a) Design of the microfluidic device and image of the actual device. The schematic depicts the cross-section view and experiment setup (left part) and the isometric view of a single-chamber of PDMS microfluidic device is shown in the insert image (right part). The device contains three layers. The bottom layer consists of an array of small circular (150 μm deep, 500 μm diameter) wells that help immobilize the islets exposed to flow. The next layer is a large circular well (3 mm deep, 7 mm diameter) that encompasses the array of the tiny wells and the top-most layer is a rectangular microchannel (500 μm deep, 2 mm wide) that provides access to these wells. (b) Plots of fluorescence intensity versus time across different regions in the perfusion chamber during the perfusion (flow rate of 1 mL/min) of DI water for 30 s followed by fluorescein isothiocyanate (2 μM FITC) for 60 s, and finally flushing out the fluorescein with DI water (intensity values are area averages of $n = 3$ scans at a region of interest).

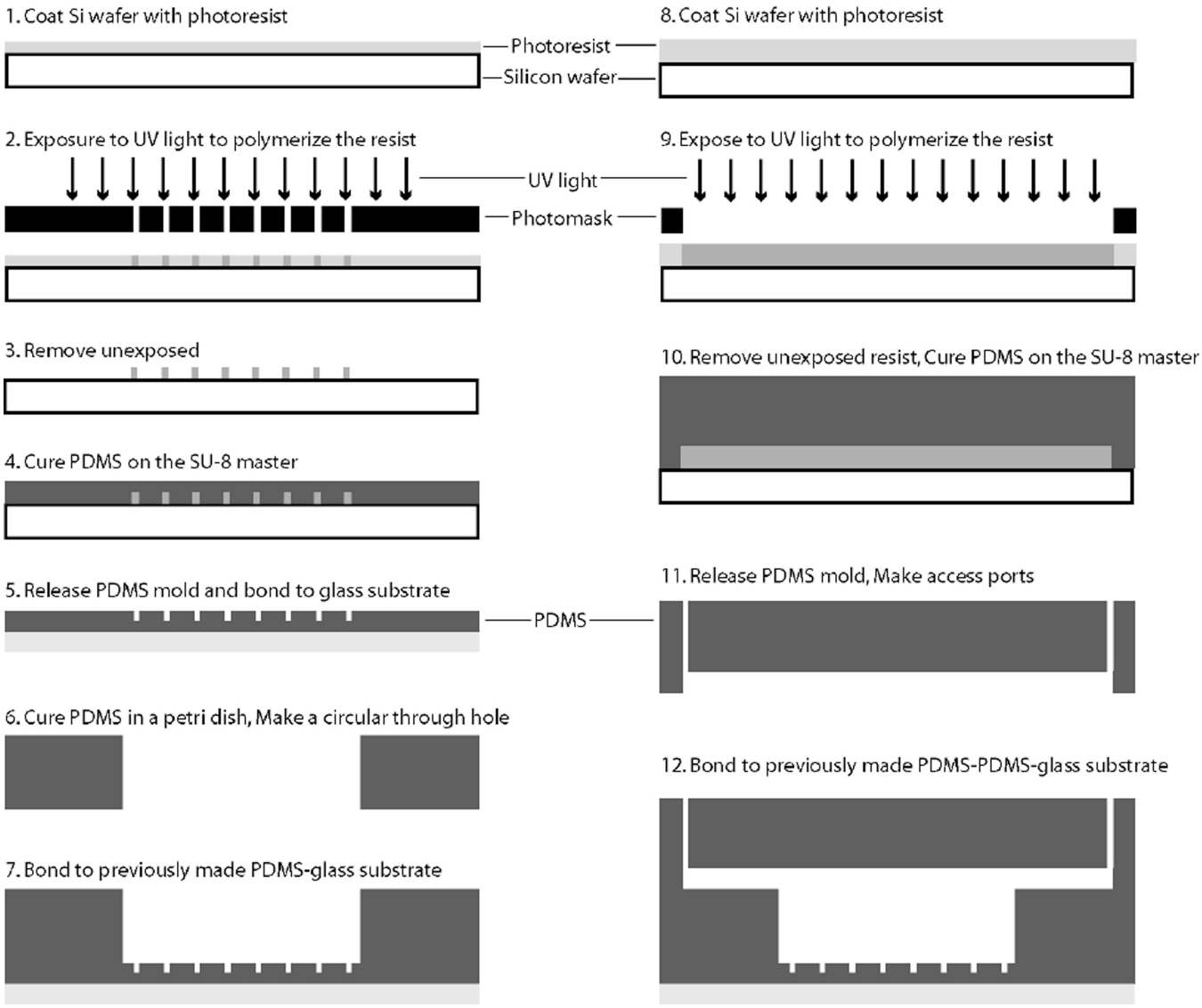

Figure 2.

Fabrication process flow for the microfluidic perfusion device. Standard SU8 lithography was used to create the masters for the array of small wells and the rectangular channels. The microfluidic device contains three layers of PDMS.

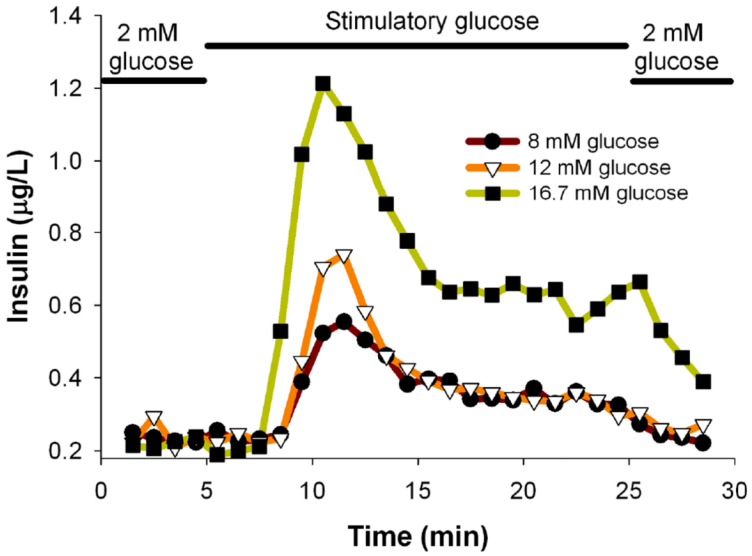

(a)

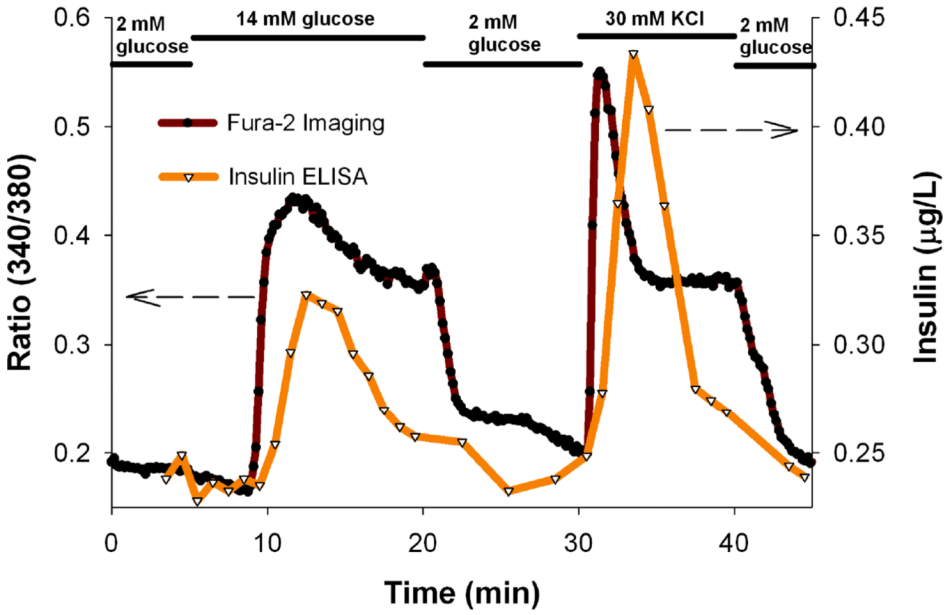

(b)

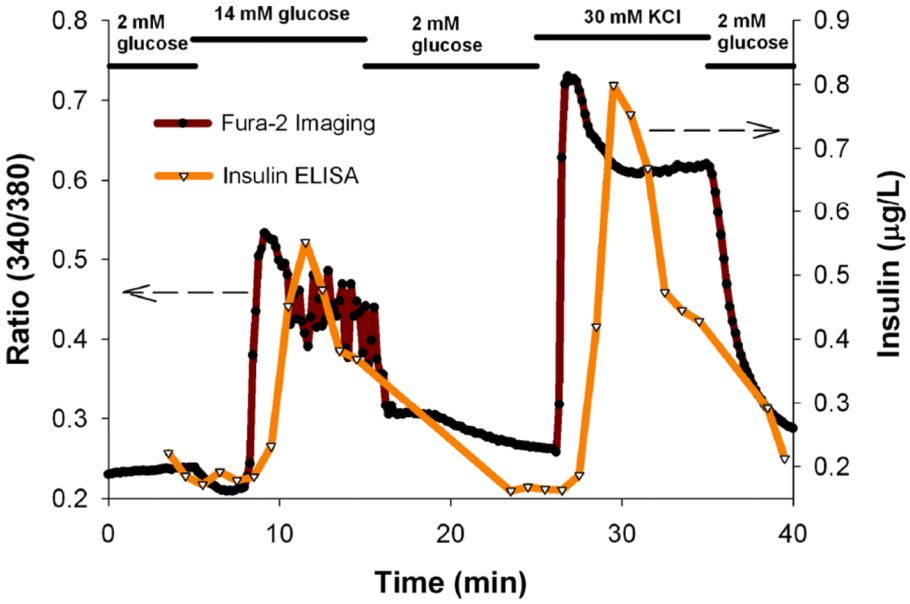

(c)

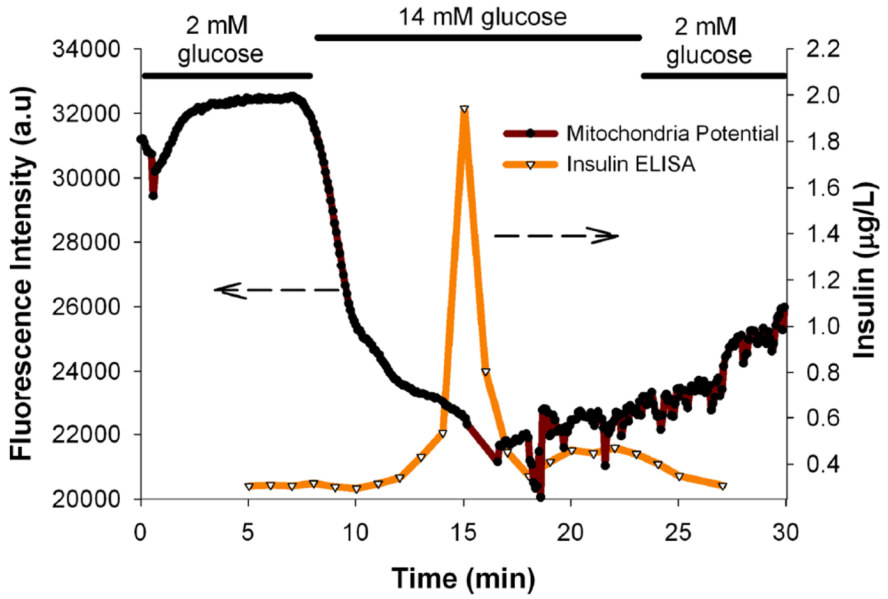

(d)

Figure 3.

(a) Temporal insulin secretion profiles of mouse islets perfused with basal and different stimulatory glucose solutions, (b) Temporal insulin secretion and $[Ca^{2+}]_i$ [indicated by Fura-2 ratio of the fluorescence intensities (340/380 nm)] profiles of C57/B6 mice islets perfused with basal and stimulatory glucose, KCl solutions, (c) Temporal insulin secretion and $[Ca^{2+}]_i$ [indicated by Fura-2 ratio of the fluorescence intensities (340/380 nm)] profiles of BALB/c mice islets perfused with basal and stimulatory glucose, KCl solutions, (d) Temporal insulin secretion and mitochondrial membrane potential profiles (indicated by fluorescence intensity of Rh123) of the mouse islets perfused with basal and different stimulatory glucose solutions. In all the experiments, 25 mouse islets were loaded per

perfusion chamber. These are results from single representative experiments with $n = 3$ replicates at each point for Fura-2 ratios and Rh123 intensities.

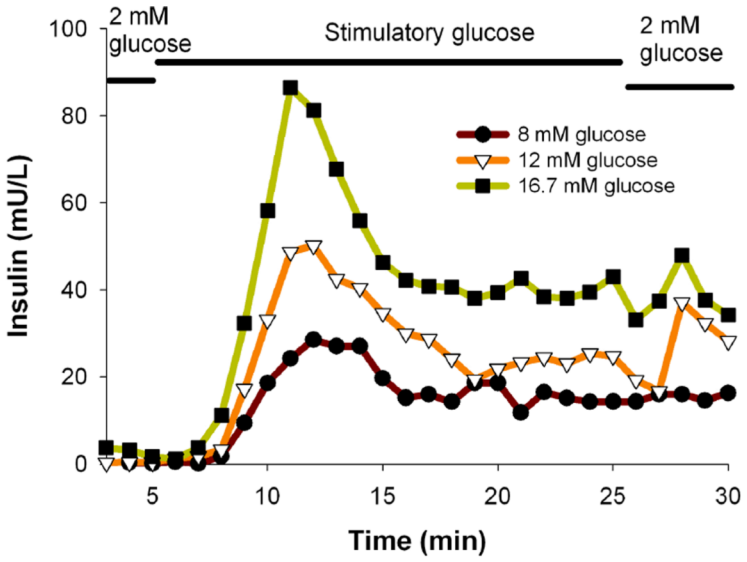

(a)

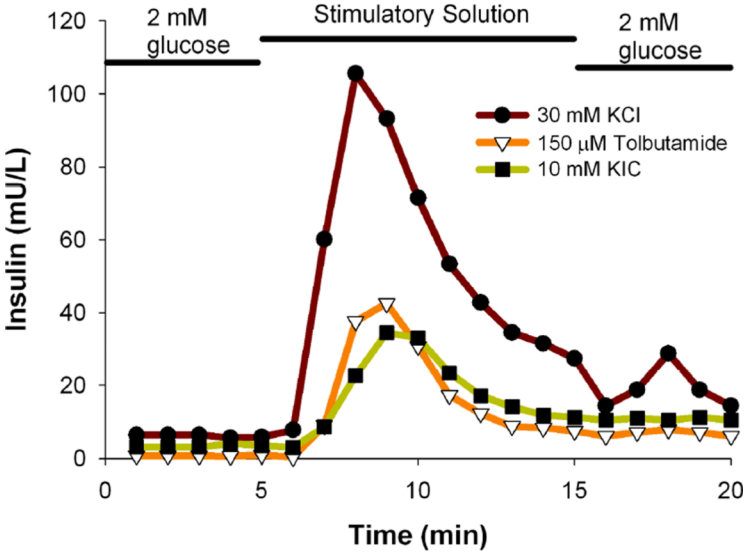

(b)

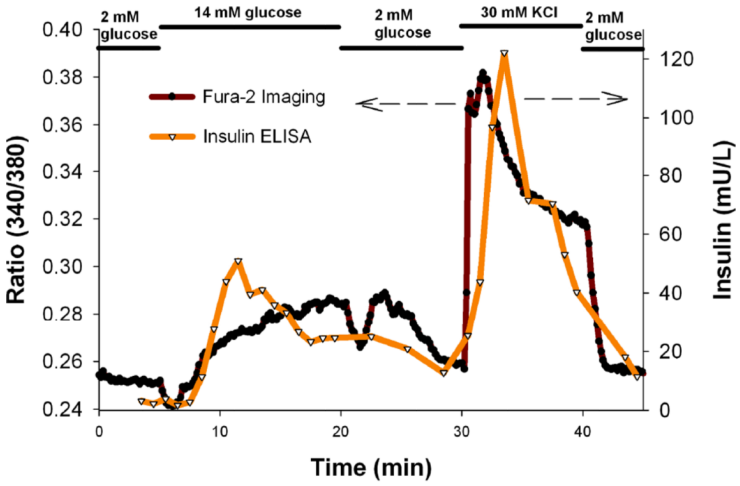

(c)

Figure 4.

(a) Temporal insulin secretion profiles of human islets perfused with basal and different stimulatory glucose solutions, (b) Temporal insulin secretion profiles of human islets perfused with basal and different secretagogue (KCl, TB, KIC) solutions, (c) Temporal insulin secretion and $[Ca^{2+}]_i$ [indicated by Fura-2 ratio of the fluorescence intensities (340/380 nm)] profiles of human islets perfused with basal and stimulatory glucose, KCl solutions. In all the experiments, 100 human islets were loaded per perfusion chamber. These are results from single representative experiments with $n = 3$ replicates at each point for Fura-2 ratios.

Table 1

Area under the curve (AUC) for insulin levels under 2 mM basal glucose (KRB2) followed by stimulation with 8, 12, 16.7 mM stimulatory glucose, and again under KRB2 in human islets (100 islets) from different human pancreatic isolation batches. These are results from single representative experiments for each isolation batch.

	AUC-8 mM			AUC-12 mM			AUC-16.7 mM		
Batch #	**KRB2**	**8 mM**	**KRB2**	**KRB2**	**12 mM**	**KRB2**	**KRB2**	**16.7 mM**	**KRB2**
1	0.79	104.10	15.52	38.43	197.20	17.95	1.45	165.20	21.19
2	0.21	188.40	17.07	0.71	201.40	4.71	0.24	193.90	12.65
3	0.13	293.40	1.61	11.42	480.40	35.88	26.70	802.10	24.41
4	0.00	105.00	4.11	1.87	94.17	4.88	0.39	171.60	3.10
5	2.48	101.20	8.83	1.41	360.00	8.07	5.33	420.80	38.14
6	0.17	105.90	7.80	4.70	196.20	14.32	0.32	160.10	23.50

Table 2

Area under the curve (AUC) for insulin levels under 2 mM basal glucose (KRB2) followed by stimulation with 30 mM KCl, 150 μM TB, 10 mM KIC, and again under KRB2 in human islets (100 islets) from different human pancreatic isolation batches. These are results from single representative experiments for each isolation batch.

	AUC-30 mM KCl			AUC-150 μM TB			AUC-10 mM KIC		
Batch #	KRB2	KCl	KRB2	KRB2	TB	KRB2	KRB2	KIC	KRB2
2	23.96	370.20	18.38	17.86	42.93	5.38	ND	ND	ND
3	12.33	312.60	13.47	29.03	168.50	9.57	ND	ND	ND
4	31.22	108.00	11.81	0.00	16.07	28.37	7.06	53.37	2.53
5	1.03	440.10	40.36	0.14	167.50	5.58	1.11	145.90	18.70
6	0.85	30.01	0.76	0.17	73.61	7.51	ND	ND	ND

Table 3

Area under the curve (AUC) for FURA-2 ratio (representing $[Ca^{2+}]_i$) and insulin levels under 2 mM basal glucose (KRB2), next by stimulation with 14 mM stimulatory glucose, under KRB2, followed by stimulation with 30 mM KCl, and finally in KRB2 in human islets (100 islets) from different human pancreatic isolation batches. These are results from single representative experiments for each isolation batch with $n = 3$ replicates at each point for Fura-2 ratios.

	AUC-FURA2					AUC-Insulin ELISA				
Batch #	**KRB2**	**14 mM**	**KRB2**	**KCl**	**KRB2**	**KRB2**	**14 mM**	**KRB2**	**KCl**	**KRB2**
1	0.13	1.80	0.42	1.56	0.14	2.26	82.40	5.28	140.60	29.03
2	0.21	0.65	0.12	1.43	0.08	0.05	40.56	2.54	154.50	2.31
5	0.00	0.17	0.03	0.51	0.05	0.71	89.40	9.41	210.00	0.10
6	0.01	0.35	0.11	0.82	0.27	0.88	375.50	58.06	263.20	3.33
7	0.01	0.16	0.05	0.20	0.03	1.43	125.00	2.18	94.36	7.61